Jurnal Teknologi

Full Paper

MITRAGYNA SPECIOSA DYE SENSITISER AS THE LIGHT-HARVESTING MOLECULES FOR DYE-SENSITISED SOLAR CELLS

Azlina A. K.[a], M. H. Mamat[b], Che Soh, Z. H.[a], M. F. A. Rahman[a], N. A. Othman[a], Marina M.[c], Syarifah Adilah M. Y.[d], M. H. Abdullah[a]

[a]Faculty of Electrical Engineering, Universiti Teknologi MARA Cawangan Pulau Pinang, Permatang Pauh, Pulau Pinang, Malaysia
[b]NANO-ElecTronic Centre (NET), School of Electrical Engineering, College of Engineering, Universiti Teknologi MARA, 40450 Shah Alam, Selangor, Malaysia
[c]Department of Computer and Mathematical Sciences, UiTM Cawangan Permatang Pauh, Pulau Pinang, Malaysia
[d]Department of Applied Sciences, UiTM Cawangan Permatang Pauh, Pulau Pinang, Malaysia

Article history
Received
1 June 2022
Received in revised form
9 October 2022
Accepted
26 October 2022
Published Online
26 December 2022

*Corresponding author
hanapiah801@uitm.edu.my

Graphical abstract

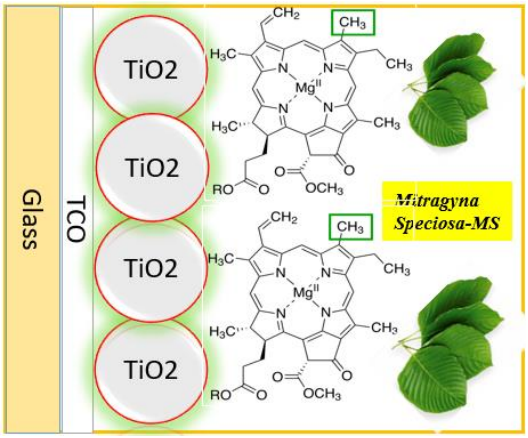

Abstract

In this study, natural dye sensitisers derived from ketum (Mitragyna speciosa-MS), spinach (Spinacia oleracea-SO), curry (Murraya koenigii-MK), papaya (Carica papaya-CP), and henna (Lawsonia inermis-LI) were investigated for dye-sensitised solar cells (DSSCs). Ultraviolet-Visible Spectroscopy (UV-Vis), Fourier Transform Infrared spectroscopy (FTIR), Open-Circuit Voltage Decay (OCVD) and Current to Voltage (I-V) were used to analyse the natural dye and the fabricated DSSC. It was observed that all dye solutions contain the majority of important functional groups of chlorophyll-based sensitisers, which is crucial for the dye-to-TiO_2 (Titanium (II) Oxide) attachment, making them suitable sources of energy harvesting pigments. In this regard, the dye pH and chemical bonding of the respective dyes play a significant role that contribute to the overall performance of the DSSCs. It was discovered that a dye based on MK provided the best DSSC performance. This is because MK-based dye has higher content of functional groups, an optimal pH, and the slowest properties of back electron recombination among the OCVD measurements. Because of the combination of these properties, the open-circuit voltage (V_{OC}), short-circuit current density (J_{SC}), and power conversion efficiency (PCE) values have been determined to be 0.58 V, 2.48 mA/cm^2, and 0.47%, respectively.

Keywords: DSSC, chlorophyll, PCE, natural dye, pH, OCVD

Abstrak

Dalam kajian ini, pemeka pewarna semulajadi yang diperoleh daripada ketum (Mitragyna speciosa-MS), bayam (Spinacia oleracea-SO), kari (Murraya koenigii-MK), betik (Carica papaya-CP), dan inai (Lawsonia inermis-LI) telah disiasat untuk sel solar peka pewarna (DSSC). Spektroskopi

Ultraviolet-Visible (UV-Vis), Fourier Transform Infrared spectroscopy (FTIR), Open-Circuit Voltage Decay (OCVD) dan Current to Voltage (I-V) telah digunakan untuk menganalisis pewarna semula jadi dan DSSC yang direka. Telah didapati bahawa semua larutan pewarna mengandungi majoriti pigmen penting dan kumpulan berfungsi asas pemeka berasaskan klorofil, yang penting untuk lampiran pewarna-ke-TiO_2, menjadikannya sumber pigmen penuaian tenaga yang sesuai. Dalam hal ini, pH pewarna dan ikatan kimia bagi pewarna masing-masing memainkan peranan penting yang menyumbang kepada prestasi keseluruhan DSSC. Telah didapati bahawa pewarna berasaskan MK memberikan prestasi DSSC yang terbaik. Ini kerana pewarna berasaskan MK mempunyai kandungan kumpulan berfungsi yang baik, pH yang optimum, dan sifat penggabungan semula elektron aliran belakang yang paling perlahan antara pengukuran OCVD. Disebabkan gabungan sifat-sifat ini, nilai voltan litar terbuka (V_{OC}), ketumpatan arus litar pintas (J_{SC}), dan kecekapan penukaran kuasa (PCE) telah ditentukan sebagai masing-masing 0.58 V, 2.48 mA/cm^2, dan 0.47%.

Kata kunci: DSSC, klorofil, kecekapan penukaran kuasa (PCE), pewarna semulajadi, pH, OCVD

1.0 INTRODUCTION

Since its discovery by Gratzel and colleagues in 1991, the DSSC has emerged as a promising photovoltaic device due to its cost-effective production methods, flexibility and transparency when compared to the conventional silicon-based photovoltaic devices [1]. The fabrication of DSSCs requires a number of essential components, including dye sensitisers, transparent conductive oxide (TCO), and TiO_2 photoelectrodes. It was determined that the most important dyes for the production of DSSC were inorganic dyes such as ruthenium-based (Ru-based) dyes. On the other hand, because of the composition of their make-up, they are hazardous to human health, extremely costly (because ruthenium is a rare metal), and challenging to purify [2]. Because of this, organic dyes have garnered a lot of attention due to their high absorption in the visible region, their ease of sample preparation, their low production costs, and their friendliness to the environment (they contain no contaminants and do not require additional refining or purification) [3].

Plants are one of the primary sources of dyes, which have been divided into four classes based on their biosynthesis basis and standard structure: chlorophyll-a and chlorophyll-b, anthocyanins, flavonoids, and carotenoids [4]. A new solar cell using chlorophyll molecules solely for all critical stages, such as light-harvesting, exciton diffusion, exciton dissociation, and charge transfer, is strongly suggested by the diverse physical features of chlorophyll. These all-chlorophyll solar cells may be able to tackle both our energy shortfall and environmental pollution issues at the same time, given the abundance of chlorophyll on our planet [5].

In our previous research, we reported the use of a novel dye additive that was utilised in the fabrication of a chlorophyll-based DSSC extracted from MS leaf [6]. In the meantime, we aim to evaluate and compare the properties and performance of the novel dye sensitiser MS with four other chlorophyll-based dye sensitisers derived from CP, LI, SO, MK. It is essential to conduct such research in order to evaluate the capabilities of this novel sensitiser in comparison to those of other chlorophyll sensitisers fabricated in the same laboratory. Since the other primary components of a DSSC, such as the transparent conduction oxide (TCO), the thickness of the TiO_2 photoelectrode, and the electrolytes, are fixed. Therefore, the primary reason for the difference in the performance can be attributed to the particular dye sensitiser that is employed. All DSSCs were tested for their optical, chemical, and electrical properties to determine the best photovoltaics conversion efficiency (PCE) among the cells.

2.0 EXPERIMENTAL

The preparation of Indium tin oxide (ITO) and porous TiO_2 photoelectrode was based on our group work as described in [6]. Meanwhile, for natural dye preparation, five different natural green dyes namely MS, SO, MK, CP and LI were washed with distilled water. Then, 10 g of each plant leaves was ground using a blender. The ground leaves were then soaked with 30 mL methanol (97%, R&M) for 2 hours. The solutions were filtered to remove any residue using a paper filter (Whatman No. 40). The comparable fresh leaves and their respective extracted dye solutions are shown in Figure 1.

The conducting side of the ITO counter electrode was created with a 2B pencil with carbon graphite lead (Faber Castell) as the catalyst layer [7], and the electrolyte was made by combining 0.05 M Iodine (I_2-Sigma Aldrich), 0.5 M Tetrabutylammonium Iodide

(TBAI-Sigma Aldrich), and 10 mL acetonitrile. DSSC was assembled by sandwiching the electrolytes between the TiO_2 photoanode and graphite counter electrode. Surface morphology and elemental composition were studied using a Field Emission Scanning Electron Microscope (FESEM-NOVA NANOSEM 450) and Energy Dispersive X-Ray (EDX) spectroscopy for characterization. The functional groups of the dye solutions were then examined using Fourier Transform-Infrared (FTIR- Thermo Scientific Nicolet 6700; software: OMNIC 8) and the adsorption was evaluated using Ultraviolet Visible spectrophotometer (UV-Vis-Lambda 25, Perkin Elmer). Photovoltaic current to voltage (I-V) measurements of DSSCs (Keithley 4200 SCS) were performed under LED (Light-emitting diode) light source to investigate the photo conversion efficiency of DSSCs.

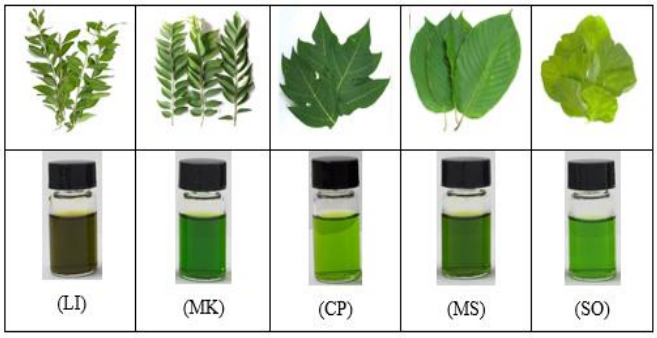

Figure 1 Fresh leaves and the extracted dyes solution of (a) henna (*LI*), (b) curry (*MK*), (c) papaya (*CP*), (d) ketum (*MS*), and (e) spinach (*SO*)

3.0 RESULTS AND DISCUSSION

3.1 Surface Morphology FESEM/ EDX and XRD

The morphology and structural images of TiO_2 nanoparticles were characterized by Field Emission Scanning Electron Microscope (FESEM) as depicted in Figure 2 (a). Using a 500 nm scale TLD (Through-the-lens detector) detector, it can be observed that the electrode is made up of nanoscale TiO_2 with a high surface area and high porosity. It was suggested that the nucleation and conjoining of microscopic particles are responsible for the development of such porous structures [8]. It is the mesoporous TiO_2 layer that aids in the increased adsorption of dye molecules, as well as the increased penetration into the TiO_2 layer by the electrolyte [9].

The crystalline phase of the TiO_2 nano-powder deposited on ITO was investigated with X-ray Diffraction (XRD), and the results are depicted in Figure 2 (b). The TiO_2 photoelectrode was analyzed in the 2 theta =10°–80° range. The presence of sharp Bragg peaks indicates that the material has a highly crystalline structure, which corresponds to peaks indexed to (101), (103), (200), (201), and (204). According to the standard diffraction card, these peaks directly correlate to the tetragonal configuration of pure anatase phase TiO_2 nanoparticles (JCPDS No. 21-1272). In addition to this, several weak peaks connected to thin-film ITO were seen at (222), (440), and (662). Figure 2 (c) depicts the EDX spectrum of TiO_2 particles. The spectrum features two significant peaks of Titanium (Ti) and Oxygen (O). As presented in Table 1, the weight percentages of Ti and O are 58.17% and 41.83%, respectively. This indicates the presence of TiO_2 nanoparticles that are free of foreign impurities [10].

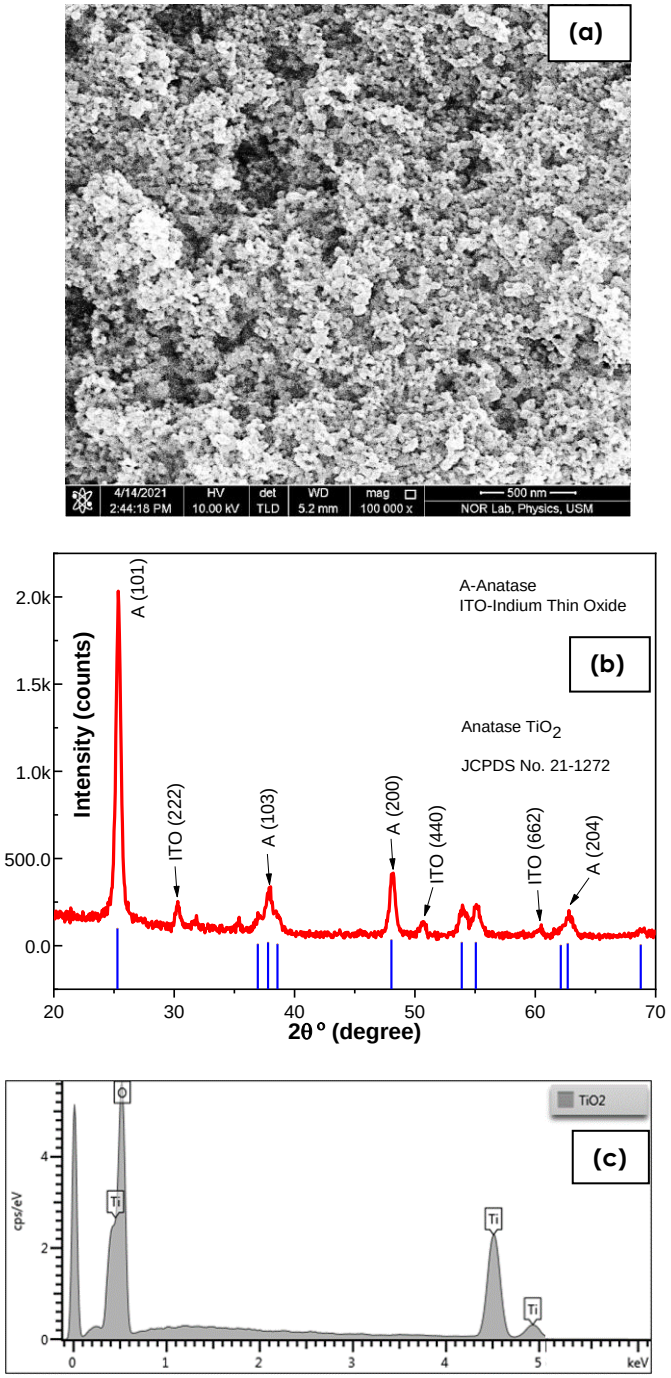

Figure 2 (a) FESEM image of porous TiO_2 photoelectrode, (b) XRD pattern of TiO_2 nanoparticle, and (c) EDX spectra of TiO_2 photoelectrode

Table 1 EDX details of TiO_2

TiO_2		
Elements	Atomic %	Weight%
O	68.28	41.83
Ti	31.72	58.17
Total	100	100

3.2 Ultraviolet-Visible Spectroscopy (UV-Vis)

The UV-Vis absorption spectra of MS, CP, LI, SO, and MK dye solutions are shown in Figure 3. It can be observed that, all dyes exhibited a similar pattern of absorption peaks between 400 nm and 800 nm. In addition, a tiny peak between 460 and 500 nm can be noticed in all dye solutions. The peaks detected between 460 nm and 470 nm are probably caused by the presence of small amount of chlorophyll-b in the extracted dye [11]. As a result, the spectra of all dye solutions reveal a pattern with two primary peaks. These patterns are associated with dominant peaks of chlorophyll-a and chlorophyll-b of green leaves [12]. Hence, all dye solutions contain the same types of pigment, which are dominated by chlorophyll-a and chlorophyll-b pigments.

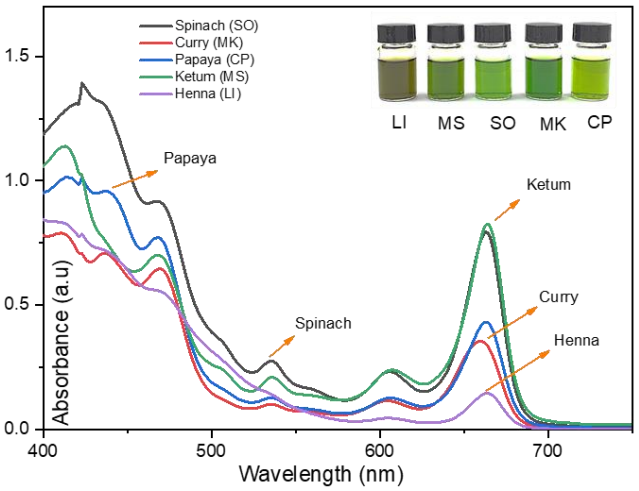

Figure 3 Optical absorption spectra of five different natural dyes extracted with methanol

It was recorded that the pH values of the LI, MS, SO, MK, and CP dyes were 5.32, 5.21, 6.53, 6.36, and 7.22, respectively. It can be noticed that the changes in the pH level have altered the green colour appearance of the dye solution, as shown in Figure 3. The variation in colour was attributed to the pH status of each solution. It was reported that the lower the pH, the higher the concentration of dissociated hydrogen ions and the greater the possibility of substitution [13]. This suggests that the rate of colour deterioration was faster in lower pH (acidic than in higher pH solutions, alkaline), because the rate of substitution of the magnesium core of the porphyrin ring reduces as the pH rises [14]. This also indicates that the pheophytinization process (two hydrogen ions replacing the magnesium ion found in the centre of the porphyrin ring under the influence of pH) is closely linked to the protein component of the prosthetic group (cofactor chlorophyll) [15]. Thus, it was determined that the pH values of SO, MK, and CP which were close to alkaline to be the optimal pH conditions for dye adsorption on TiO_2 surface owing to less substitution of magnesium ions in the porphyrin ring [16].

3.3 Transform Infrared (FTIR) Analysis

The FTIR spectra of the five different dye solutions are shown in Figure 4. In the instance of LI dye solution, it contains a range of chemicals including flavonoids, gallic acid, lawsone and tannin. The infrared spectrum for LI reveals two primary anticipated frequency sections within the band of interest, namely hydroxyl (OH) and carbonyl (C=O). The stretching vibration of the hydroxyl group, was detected at the first lawsone aromatic ring, which is attributed to the hydroxyl group of lawsone (2-hydroxy, 1-4-napthoqunone) [17]. Stretching absorption at 3310 cm^{-1} corresponds to the vibration of the related O-H bond. Meanwhile, the bending and stretching vibrations of C–H are depicted at peaks 2950 cm^{-1} and 2830 cm^{-1}, and the carbonyl group in lawsone stretching vibration at 1640 cm^{-1}. Finally peaks at 1440 cm^{-1} and 1400 cm^{-1} signify the aromatic C=C group [18].

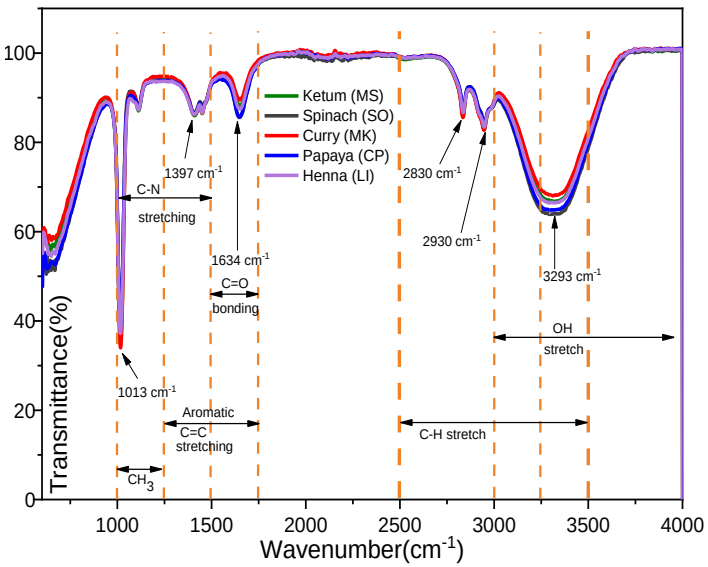

Figure 4 FTIR spectra with respect to various natural chlorophyll-based dyes

Again, the presence of hydroxyl and carbonyl in CP dye solution can be seen at 3290 cm^{-1} and 1634 cm^{-1}, respectively. As seen, MK leaves have rich sources of polyphenols, flavonoids, and glycosides [19]. MK has exhibited a broad absorption band at 3290 cm^{-1}, which has been ascribed to the O-H stretch in the alcohol group [20]. Meanwhile, peaks at 2830 cm^{-1} and 2930 cm^{-1} correspond to C-H stretching in alkanes. [20]. Following that, the peak at 1630 cm^{-1} was identified as aromatic C=C stretching [21].

It has been reported that the hydroxyl (O-H) and carbonyl (C=O) groups of the molecule's sensitisers may aid dye-sensitised solar cells in converting light more effectively into electrons [22]. In addition, asymmetric C-H bending of the methyl and methylene groups at 2830 cm^{-1} and 2930 cm^{-1} was slightly higher than the rest of the sensitisers, therefore there might be the possibility of higher dye adsorption on the TiO_2 photoelectrode later on which can give rise to the overall performances of the MK-based cell. Hence, MK cell has the highest efficiency compared with other cells.

The broad FTIR peak of the SO sample at 3290 cm^{-1} corresponds to the O-H stretching vibration due to the presence of methanol [23]. Meanwhile, peaks found at 2830 cm^{-1} and 2930 cm^{-1} were corresponding to the C-H bending. Then, the 1630 cm^{-1} peak corresponds to C=O (carbonyl). Meanwhile, MS dye solution exhibited a prominent peak at 3293 cm^{-1}, which can be attributed to O-H stretch. Finger print peaks can be identified between the range 600 cm^{-1} and 1100 cm^{-1} for all organic dyes. At pH 5–6, however, the dye's O–H group and C–C stretching content decreased, possibly as a result of the environment's high (alkaline) pH damaging the groups [24].

3,4 Photovoltaic Characteristics

Figure 5 (a) depicts the photocurrent voltage characteristics of various DSSCs cells, along with an inset image displaying five cells that were used for the measurement. The parameters of the photovoltaic characteristics are summarized in Table 2. Based on the data, the MK cell had the highest PCE of 0.47%. Meanwhile, the PCE of CP, SO, LI, and MS DSSC cells are 0.19%, 0.16%, 0.09%, and 0.11%, respectively. Notably, the MK and MS dyes have greater V_{OC} values than the other cells, at 0.58 V and 0.56 V, respectively. It is worth noting that the fill factor of 42.66% obtained by employing MS as sensitiser is the highest among other organic dyes. In this study, the highest efficiency of the MK cell with 0.47% of PCE is seen to be attributed to the larger short-circuit current induced by appropriate dye adsorption and less back recombination witnessed by OCVD measurement (Figure 5 (b)). In other words, increasing dye-loading leads to higher DSSC photocurrent and, as a result, higher efficiency [25, 26].

Additionally, it is possible that the superior performance of MK-based cells is due to their higher antioxidant properties, which allow them to restore and rejuvenate their chlorophyll molecules inside the cell for a longer period of time. It has been reported that MK are anti-carcinogenic, enzymatic antioxidant effect, hypoglycemic, and antimicrobial [27]. Antioxidants that are enzyme-based, accomplish their work by inhibiting, modulating, and ultimately eliminating the effects of free radical reactions. Through a series of chemical reactions, the antioxidant enzymes turn potentially harmful oxidative products into harmless water [28].

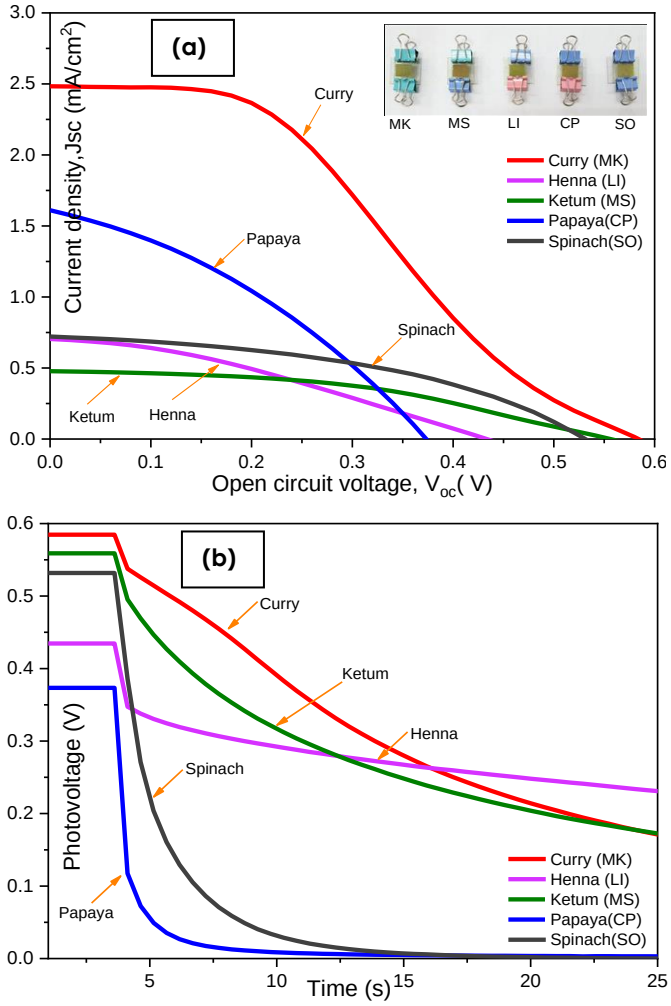

Figure 5 (a) Photovoltaics properties of DSSCs with various dye solution (inset image: fabrication of DSSC cell of five different sensitisers), and (b) Open-circuit voltage decay (OCVD) of several DSSCs with respect to different dye solution

Table 2 Photovoltaic performances of DSSCs with respect to various natural dyes sensitiser

Type of sensitisers	Jsc (mA/cm²)	V_{OC} (mV)	FF (%)	η (%)
MS	0.48	560	42.66	0.11
CP	1.61	370	32.36	0.19
LI	0.71	430	29.46	0.09
SO	0.73	530	40.18	0.16
MK	2.48	580	32.90	0.47

The oxidative stress is caused by a variety of pathophysiological conditions and oxidative products such as reactive oxygen species (ROS) [29]. These ROS are able to interact with oxygen-dependent mechanisms, leading to the destruction of microorganisms and biological molecules like DNAs, proteins, and lipids, and subsequently causing chemical damage to these molecules [30, 31].
Meanwhile, when compared to other organic dyes, LI-based cell has the lowest conversion efficiency and FF at 0.09% and 29.46%, respectively. This is most likely owing to a shortage of accessible bonds between the

dye and TiO_2 molecules, through which electrons can be transported from the excited dye molecules to the TiO_2 layer [32]. The lower FF could be ascribed to the dyes being less tightly bound to the TiO_2 network, which could result in greater recombination within the cell [33]. From the findings, it was discovered that the interaction between the sensitiser and the TiO_2 layer is critical in enhancing the energy conversion efficiency of the DSSC.

Open-circuit voltage decay was studied by monitoring the DSSC's during open-circuit voltage without illumination under open-circuit conditions [34]. This technique can be used to trace the progressive loss of photo-generated electrons due to recombination by measuring the transient V_{OC} as a function of time after the light is turned off. When the light is switched off with a shutter under a stable voltage, V_{OC} decays faster due to electron recombination, which is related to the electron lifespan [35]. As illustrated in Figure 5 (b), due to the faster V_{OC} decay rate, the recombination kinetics of the photogenerated electrons in the CP cell became faster, indicating that CP cell has the shortest lifetime compared with other cells. The V_{OC} decay is slower in the cell constructed with MK dye, resulting in slower electrons recombination dynamics and a longer lifetime in the cell constructed with MK dye. Therefore, the MK cell has the highest number of photogenerated electrons that can survive from the back recombination process, and finally this contributes to the highest conversion efficiency PCE.

4.0 CONCLUSION

Five distinct chlorophyll-based organic dye sensitisers were successfully investigated in this work, and the results were thoroughly discussed as the above. The investigations into the dyes using UV–Vis spectroscopy and FTIR spectroscopy demonstrated that all dyes are suitable to be used as sensitiser due to their visible absorption of chlorophyll pigment and the presence of functional groups that can bond with the TiO_2. Among their functional groups are hydroxyl (OH) and carbonyl (C=O) which play vital parts for the dye-to-TiO_2 attachment of the cell. In addition, the optimal pH condition (which leans toward alkaline) for the chlorophyll-based cell is found to be one of the factors associated with the observed improvement in the PCE. This finding was made possible by the fact that chlorophyll thrives in an alkaline environment. One of the other most obvious properties that contributed to the higher PCE was the lower back recombination of the cell, which was measured by OCVD. This was one of the properties that contributed to the higher PCE. The MK-based cell displayed the slowest back recombination of all the cells, which in turn contributed to the highest J_{SC} and V_{OC} values. With all of its integrated properties, the MK cell demonstrated the highest DSSC efficiency possible, which came in at 0.47%. In conclusion, organic dyes are a promising alternative because they are simple to produce, readily available in a wide variety of locations, and affordable. When combined with DSSC, it possesses the potential to serve as a good sensitiser. In addition, when all of the other components of the DSSC were assumed to be constant throughout the cells (the thickness of the TiO_2 layer, the electrolyte, and the counter electrode), the MK-based sensitiser outperformed the MS-based sensitiser by a factor of three in terms of its performance and PCE.

Acknowledgement

The authors would like to thank the Ministry of Higher Education of Malaysia (MOHE) for funding this research through Fundamental Research Grant Scheme (FRGS-2019-1) (ID No 284362-301651). The authors would like to thank to Chemical Engineering UiTM Cawangan Pulau Pinang for their UV-Vis and FTIR equipments, as well as USM Pulau Pinang for providing their FESEM machine.

References

[1] M. Grätzel and B. O'Regan. 1991. A Low-cost, High-efficiency Solar Cell based on Dye-sensitized Colloidal TiO_2 films. *Nature*. 353(6346): 737-740. Doi: 10.1038/353737a0.

[2] M. Rekha, M. Kowsalya, S. Ananth, P. Vivek, and R. M. Jauhar. 2019. Current–voltage Characteristics of New Organic Natural Dye Extracted from Terminalia Chebula for Dye-sensitized Solar Cell Applications. *J. Opt.* 48(1): 104-112. Doi: 10.1007/s12596-018-0507-5.

[3] M. Z. Iqbal, S. R. Ali, and S. Khan. 2019. Progress in Dye Sensitized Solar Cell by Incorporating Natural Photosensitizers. *Sol. Energy*. 181: 490-509. Doi: https://doi.org/10.1016/j.solener.2019.02.023.

[4] H. El-Ghamri, T. El-Agez, S. Taya, M. Abdel-Latif, and A. Batniji. 2014. Dye-sensitized Solar Cells with Natural Dyes Extracted from Plant Seeds. *Mater. Sci.* 32(4): 547-554. Doi: 10.2478/s13536-014-0231-z.

[5] K. Wongcharee, V. Meeyoo, and S. Chavadej. 2007. Dye-sensitized Solar Cell using Natural Dyes Extracted from Rosella and Blue Pea Flowers. *Sol. Energy Mater. Sol. Cells*. 91(7): 566-571. Doi: 10.1016/j.solmat.2006.11.005.

[6] A. A. Khan *et al.* 2022. Magnesium Sulfate as a Potential Dye Additive for Chlorophyll-based Organic Sensitiser of the Dye-sensitised Solar Cell (DSSC). *Spectrochim. Acta Part A Mol. Biomol. Spectrosc*. 274: 121140. Doi: 10.1016/j.saa.2022.121140.

[7] F. Hölscher, P. R. Trümper, I. Juhász Junger, E. Schwenzfeier-Hellkamp, and A. Ehrmann. 2019. Application Methods for Graphite as Catalyzer in Dye-sensitized Solar Cells. *Optik (Stuttg)*. 178(August 2018): 1276-1279. Doi: 10.1016/j.ijleo.2018.10.123.

[8] G. N. 2014. Natural Dye Sensitized Nanocrystalline Tio2 Thin Films for Solar Cell Applications. Anna University, Chennai, India.

[9] A. Zdyb and E. Krawczak. 2021. Organic Dyes in Dye-sensitized Solar Cells Featuring Back Reflector. *Energies*. 14(17). Doi: 10.3390/en14175529.

[10] H. Chang, M.-J. Kao, T.-L. Chen, C.-H. Chen, K.-C. Cho, and X.-R. Lai. 2013. Characterization of Natural Dye Extracted from Wormwood and Purple Cabbage for Dye-Sensitized Solar Cells. *Int. J. Photoenergy*. 1-8. Doi: 10.1155/2013/159502.

[11] O. Adedokun, Y. K. Sanusi, and A. O. Awodugba. 2018. Solvent Dependent Natural Dye Extraction and Its

Sensitization Effect for Dye Sensitized Solar Cells. *Optik (Stuttg)*. 174: 497-507. Doi: 10.1016/j.ijleo.2018.06.064.
[12] Lakna. 2017. Difference between Chlorophyll A and B Difference Between Chlorophyll A and B Main Difference-Chlorophyll A vs Chlorophyll B. *Pediaa*. April [Online]. https://www.researchgate.net/publication/316584030.
[13] W. Van Lierop. 2018. Soil pH and Lime Requirement Determination. *Soil Test. Plant Anal*. 9(9): 73-126. Doi: 10.2136/sssabookser3.3ed.c5.
[14] M. I. Gunawan and S. A. Barringer. 2000. Green Color Degradation of Blanched Broccoli (Brassica Oleracea) due to Acid and Microbial Growth. *J. Food Process. Preserv*. 24(3): 253-263. Doi: 10.1111/j.1745-4549.2000.tb00417.x.
[15] P. Koli and U. Sharma. 2021. Use of Pigments Present in the Crude Aqueous Extract of the Spinach for the Simultaneous Solar Power and Storage at Natural Sun Intensity. *Adv. Energy Sustain. Res.* 2(11): 2100079. Doi: 10.1002/aesr.202100079.
[16] A. M. Humphrey. 2004. Chlorophyll as a Color and Functional Ingredient. *J. Food Sci*. 69(5). Doi: 10.1111/j.1365-2621.2004.tb10710.x.
[17] Y. Takeda and M. Fatope. 1988. New Phenolic Glucosides from Lawsonia Inermis. *J. Naural Prod.* 51(4): 725-729. Doi: 10.1021/np50058a010.
[18] M. A. Slifkin. 1973. Infrared Spectra of Some Organic Charge-transfer Complexes. *Spectrochim. Acta Part A Mol. Spectrosc.* 29(5): 835-838. Doi: https://doi.org/10.1016/0584-8539(73)80053-4.
[19] M. B. Ningappa, R. Dinesha, and L. Srinivas. 2008. Antioxidant and Free Radical Scavenging Activities of Polyphenol-enriched Curry Leaf (Murraya koenigii L.) Extracts. *Food Chem*. 106(2): 720-728. Doi: 10.1016/j.foodchem.2007.06.057.
[20] K. Elumalai, S. Velmurugan, S. Ravi, V. Kathiravan, and S. Ashokkumar. 2015. Bio-fabrication of Zinc Oxide Nanoparticles using Leaf Extract of Curry Leaf (Murraya koenigii) and Its Antimicrobial Activities. *Mater. Sci. Semicond. Process.* 34: 365-372. Doi: 10.1016/j.mssp.2015.01.048.
[21] A. M. Anton *et al.* 2019. Photoresponsive Natural Materials. *Mol. Cryst. Liq. Cryst*. 695(1): 37-44. Doi: 10.1080/15421406.2020.1723904.
[22] J. Coates. 2006. Interpretation of Infrared Spectra, A Practical Approach. *Encycl. Anal. Chem.* 1-23. Doi: 10.1002/9780470027318.a5606.
[23] F. Kabir, S. N. Sakib, and N. Matin. 2019. Stability Study of Natural Green Dye based DSSC. *Optik (Stuttg)*. 181(December 2018): 458-464. Doi: 10.1016/j.ijleo.2018.12.077.
[24] S. Suyitno, T. J. Saputra, A. Supriyanto, and Z. Arifin. 2015. Stability and Efficiency of Dye-sensitized Solar Cells based on Papaya-leaf Dye. *Spectrochim. Acta - Part A Mol. Biomol. Spectrosc*. 148: 99-104. Doi: 10.1016/j.saa.2015.03.107.
[25] Shahrul, A. M., *et al*. 2022. Synergistic Role of Aluminium Sulphate Flocculation Agent as Bi-functional Dye Additive for Dye-Sensitized Solar Cell (DSSC). *Optik.* 258. 168945.doi.org/10.1016/j.ijleo.2022.168945.
[26] S. Hao, J. Wu, Y. Huang, and J. Lin. 2006. Natural Dyes as Photosensitizers for Dye-sensitized Solar Cell. *Sol. Energy*. 80(2,): 209-214. Doi: 10.1016/j.solener.2005.05.009.
[27] M. B. Ningappa, B. L. Dhananjaya, R. Dinesha, R. Harsha, and L. Srinivas. 2010. Potent Antibacterial Property of APC Protein from Curry Leaves (Murraya koenigii L.). *Food Chem*. 118(3): 747-750. Doi: 10.1016/j.foodchem.2009.05.059.
[28] Shahidi, Fereidoon, and Ying Zhong. 2010. Novel Antioxidants in Food Quality Preservation and Health Promotion. *European Journal of Lipid Science and Technology*. 112(9): 930-940. Doi.org/10.1002/ejlt.201000044
[29] Kim, Young-Woong, and Tatiana V. Byzova. 2014. Oxidative Stress in Angiogenesis and Vascular Disease. *Blood, The Journal of the American Society of Hematology*. 123(5): 625-631. Doi.org/10.1182/blood-2013-09-512749.
[30] Dizdaroglu, Miral, *et al.* 2002. Free Radical-induced Damage to DNA: Mechanisms and Measurement. *Free Radical Biology and Medicine*. 32(11): 1102-1115. doi.org/10.1016/S0891-5849(02)00826-2.
[31] Halliwell, Barry, and John MC Gutteridge. 2015. Free Radicals in Biology and Medicine. Oxford University Press, USA.
[32] S. Hao, P. Wu, Y. Huang, and J. Lin. 2006. Natural Dyes as Photosensitizers for Dye-sensitized Solar Cell. *Sol. Energy*. 80: 209-214. Doi: 10.1016/j.solener.2005.05.009.
[33] Suyitno, A. Zainal, A. S. Ahmad, T. S. Argatya, and Ubaidillah. 2014. Optimization Parameters and Synthesis of Fluorine Doped Tin Oxide for Dye-sensitized Solar Cells. *Appl. Mech. Mater.* 575: 689-695. Doi: 10.4028/www.scientific.net/AMM.575.689.
[34] Z. Nazila and R. Rasuli. 2018. Anchored Cu_2O Nanoparticles on Graphene Sheets as an Inorganic Hole Transport Layer for Improvement in Solar Cell Performance. *Appl. Phys. A Mater. Sci. Process.* 124(12). Doi: 10.1007/s00339-018-2229-6.
[35] Shahrul, A. M., *et al*. 2022. Low-cost Coagulation Treatment of Dye Sensitizer for Improved Time Immersion of Dye-sensitized Solar Cells (DSSC). *Microelectronic Engineering*. 262: 111832. Doi.org/10.1016/j.mee.2022.111832.